Journal of Luminescence 146 (2014) 256–262

Contents lists available at ScienceDirect

Journal of Luminescence

journal homepage: www.elsevier.com/locate/jlumin

The role of FRET in solar concentrator efficiency and color tunability

Benjamin Balaban, Sage Doshay, Melissa Osborn, Yvonne Rodriguez, Sue A. Carter*

Department of Physics, University of California Santa Cruz, 1156 High Street, Santa Cruz, CA 95064, USA

ARTICLE INFO

Article history:
Received 30 December 2012
Received in revised form
30 August 2013
Accepted 18 September 2013
Available online 8 October 2013

Keywords:
Luminescent solar concentrator
Luminescent solar collector
LSC
Energy transfer
Luminescent
Foerster resonant energy transfer

ABSTRACT

We demonstrate concentration-dependent Förster-type energy transfer in a luminescent solar concentrator (LSC) material containing two high quantum yield laser dyes in a PMMA matrix. FRET heterotransfer is shown to be approximately 50% efficient in the regime of 2×10^{-3}molal acceptor dye by weight in the host polymer. The two dyes used have been well studied for solar concentrator applications: BASF's Lumogen Red 305, and Exciton Chemical Company's DCM both demonstrate desirable stability, quantum yield, and complementary absorption spectra. We demonstrate how multiple-dye LSC devices employing FRET increase the absorption of air mass 1.5 solar irradiance without affecting the self-absorption properties of the film. Color tunability may be achieved through the addition of additional absorbers while minimizing the impact on waveguide efficiency.

1. Introduction

Luminescent solar concentrators (LSCs) offer low cost improvements to building-integrated photovoltaics. An LSC generally consists of an optically transparent material with an index of refraction similar to that of glass doped or coated with a fluorescent downconversion material which absorbs solar radiation and isotropically reemits it at longer wavelengths with a high quantum yield. Thus, a certain percentage of the reemitted light is subject to total internal reflection and trapped in the waveguide. The trapped photons are then absorbed by strips of active PV material optically coupled into the waveguide in a variety of potential geometries.

The history of the LSC can be traced back at least 50 years, stemming from the development of scintillation detectors [1]. Although this work is noted for its pioneering consideration of the "fluorescent solar collector" concept in the publications of Seybold and Wagenblast [2], who later developed highly soluble and relatively stable perylene dyes specifically for solar concentrator applications, the 1976 conceptual publication of Weber and Lambe [3] is variously cited as the first published LSC concept, while several review articles [4,5]] note from the work of Batchelder et al. [6] that a 1973 NSF proposal by R.M. Lerner is considered to be the concept's unpublished introduction. In the proposal of the LSC concept by Weber and Lambe [3], the overall efficiency of an LSC device was defined as the product of three efficiencies:

$$E = Q_a \eta Q_c$$

with Q_a and η representing initial absorption of solar photon flux and fluorescence quantum yield, respectively. Thus Q_c was defined as the "collection efficiency," which takes into account geometric losses from both the initial re-emission and subsequent re-absorption and emission events, as well as losses from reflection when light travels from a relatively low refractive index waveguide into a semiconductor photovoltaic material. Given approximately equal quantum yields of all dyes, the main benefit should come from reducing the number of re-emission and absorption events and thus total escape cone and quantum yield losses.

While dye stability still remains an issue for many LSC-suitable dyes [5], some progress has been made within the past several decades with dyes such as Rhodamine [7] and Perylene dyes with the work of Seybold and Wagenblast at BASF [2]. Still, LSCs have been inherently limited in power efficiency by low absorption of the solar spectrum, self-absorption of the emitted light, and waveguide losses. While attempts have been made to improve efficiency and maintain stability by increasing absorption using quantum dots [8,9]], broadening absorption and tuning emission through dye interaction with the host environment [10], or using dipole alignment to reduce escape cone losses [11,12], the largest single loss is often the narrow absorption spectra of many proposed LSC materials [13]. Shortly after Weber and Lambe's 1976 publication, the idea of constructing multiple-dye LSC films to increase absorption was studied [14]. While the prospect of exciton transfer through resonance between a donor's fluorescence transition dipole and a corresponding transition of an

* Corresponding author. Tel.: +1 831 335 7595.
E-mail addresses: bbalaban@ucsc.edu (B. Balaban), sacarter@ucsc.edu (S.A. Carter).

0022-2313/$ - see front matter © 2013 Elsevier B.V. All rights reserved.
http://dx.doi.org/10.1016/j.jlumin.2013.09.049

acceptor (Förster-type nonradiative transfer) was immediately considered, it was estimated to play a small role in the experiments carried out by Swartz et al. [14], owing to the low concentrations used. More recent undertakings have studied the overall efficiency in an LSC system where FRET was shown to be the dominant transfer mechanism between three chromophores [15], but no discussion was made of the concentration regime at which FRET began to occur in a PMMA matrix.

Average donor–acceptor pair distance calculation can be less straightforward than what a cursory glance at Förster's well known relations suggests (Eqs. (1)–(3)). While the relations are generally used to estimate Förster-type transfer efficiency between fluorophores in fixed positions, such as those bound to specific sites on proteins and used for biolabeling [16], in a polymer matrix a distribution of distances must be considered. A further complicating matter is that a polymer LSC host matrix does not guarantee a uniform distribution of dopants, leading to quenching-pair distance relations which are nontrivial to calculate numerically [17]. Specifically, mathematical models relating dopant distributions to FRET quenching in a two-dye system have been proposed as a means of gaining insight into the morphology of porous materials such as polymers, among other things [18]. Such models require time-resolved fluorescence measurements and, in the case of [18], neglect homotransfer and consider transfers only between isolated donor–acceptor pairs – a very low concentration situation that is of limited utility when considering solar concentrator applications.

The self-absorption characteristics of planar LSC films have similarly been well studied for DCM and Lumogen F dyes specifically [13,19–21]. For any given LSC geometry, there is a tradeoff between increasing AM1.5 photon capture and the associated geometric losses from self-absorption and lowered quantum yield due to possible aggregate formation and other quenching effects. Thus, for LSC devices containing multiple fluorescent species, a knowledge of the concentration regimes at which FRET begins to occur is important to consider when optimizing dye concentrations against geometric gains.

Initial interest in solar concentrator devices was sparked in the mid- to late 1970s [4]. Oil supply shock coupled with an inflation adjusted cost per watt of PV modules around two orders of magnitude higher than today [22] motivated a search for cost effective concentration mechanisms allowing for maximal PV power output from a minimal amount of area. The considerably lower cost per watt of solar in today's market has led to a re-evaluation of the economics of LSC schemes, with recent potential application focused on cells which receive both direct and waveguide illumination and close attention is paid to installed cost per watt [23]. In these types of layouts, self-absorption of the LSC will determine the optimal arrangement of face mounted photovoltaic cells [13,23], and building integrated PV will generally require higher transparency and thus push low concentration limits for esthetic purposes. We frame our study with these considerations, and quantify concentration depending FRET experimentally in a PMMA-host planar LSC setup with a spectroscopic study of a two dye system.

2. Experimental procedure

DCM ([2-[2-[4-(dimethylamino)phenyl]ethenyl]-6-methyl-4H pyran-4-ylidene]-propanedinitrile; Exciton) and Lumogen Red 305 (BASF) were used as obtained (structures are shown in Fig. 1). Luminescent inks were prepared from a mixture of the as-received powdered dyes, polymethylmethacrylate (Spectrum Chemical Co., 350k molecular weight), and toluene. To achieve global film uniformity across a range of dye to host polymer concentrations, a standard 13.3% PMMA:toluene weight ratio was

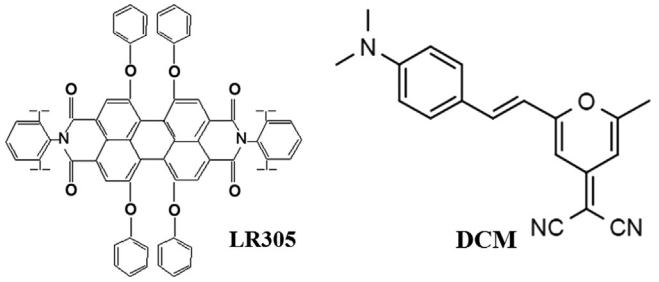

Fig. 1. Chemical structures of BASF Lumogen F Red 305, a perylene diimide and Exicton DCM, a merocyanine.

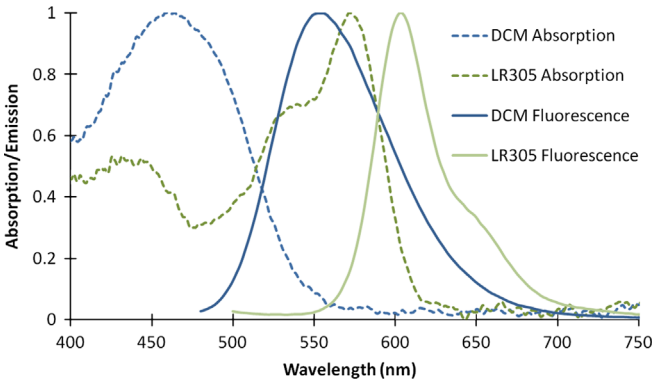

Fig. 2. Normalized absorption and emission spectra of LR305 and DCM dyes in PMMA.

established for all inks. The film deposition was performed using an Industry Tech Auto Draw III automatic drawdown machine. The machine draws a rod across a slide at constant pressure and velocity to produce a film. Film thickness was set using a single layer of Scotch 810 magic tape, in a process commonly referred to as "doctor-blading". The films were deposited on 3 in. × 1 in. quartz glass microscope slides. The films themselves were determined to be approximately 5 μm in thickness.

A Stellar Net Thin Film Measurement System, including an SL-1 Filter, a CXR-SR-25 BW-16 Spectrometer, and a Wave NIR-25 InGaAs BW Spectrometer, was used to measure absorption spectra. A Perkin-Elmer Instruments LS45 Luminescence Spectrometer was used to measure the surface emission of the films, by placing the samples in the spectrometer's "front surface" accessory. The excitation beam strikes at 60° to the film's normal, and emission is collected at 30° relative to the film normal. Film thickness measurements were determined by a Dektak profilometer and found to be in agreement with the known molar absorption coefficient from literature [21].

3. Results and discussion

BASF Lumogen Red 305 and DCM dyes fluoresce in the yellow–red visible range, with emission peaks around 604 nm and 555 nm, respectively, when embedded in a PMMA polymer matrix. Both have been considered for use in LSC applications because of their broad Stokes shifts and high quantum yields. In addition to its promising spectroscopic properties, DCM was investigated as a companion dye to Lumogen Red 305 because its absorption peak complements a dip in the absorption spectrum of LR305 (Fig. 2).

It is worth noting that DCM, like other merocyanines, is prone to solvatochromatic effects; its emission peak redshifts from approximately 550 nm to 600 nm or more, generally varying with the polarity of its host environment; the effect was noted in the

work of Batchelder et al. [19] and elsewhere, such as in Ref. [24]. The 550 nm peak emission observed in our films is characteristic of the DCM's behavior in low polarity host environments and it has been shown to have a quantum yield of 76% in PMMA [25].

LR305 has been shown to be capable of near unity quantum yield in PMMA [26]. It was similarly noted in Ref. [22] that the molecular emission spectrum of LR305 was seen to shift between 597 nm and 611 nm (with no change in quantum yield) as the excitation wavelength varied between 490 nm and 620 nm, respectively. The authors noted that this could be explained by the redshift absorption and emission of dimer or trimer aggregates contributing to emission at longer excitation wavelengths. Our attempts to replicate this effect were unsuccessful; with 0.1% LR305:PMMA 5 μm films and optical densities sufficiently low to neglect self-absorption effects [16], we observed a consistent 604 nm emission peak between 440 and 590 nm excitation with 3 nm entrance and exit slit bandwidth (Fig. 3). Differences in the experimental setup and film preparation method ("doctor-blading" a toluene:polymer:dye mixture versus casting thick molds) required us to use concentrations at least an order of magnitude greater than in Ref. [21]. Thus, it is possible that FRET homotransfer is responsible for an average effect of the fluorescence at all excitation wavelengths, although a simpler qexplanation would be differences in spectrometer calibration and the absence of the aggregates in our films – either due to differences in received dye batches, or perhaps from differences in the film preparation method.

We compared the surface emission (Fig. 4) and absorption spectra of single dye LSC films, blended LSC films, and stacked single dye films.

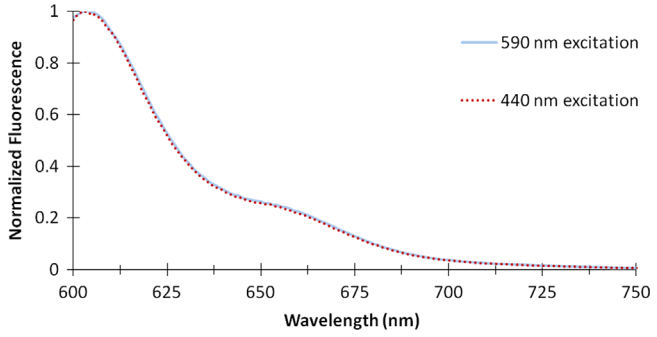

Fig. 3. Emission spectra of low optical density LR305 films in PMMA. No change in emission is observed between 440 nm and 590 nm excitation.

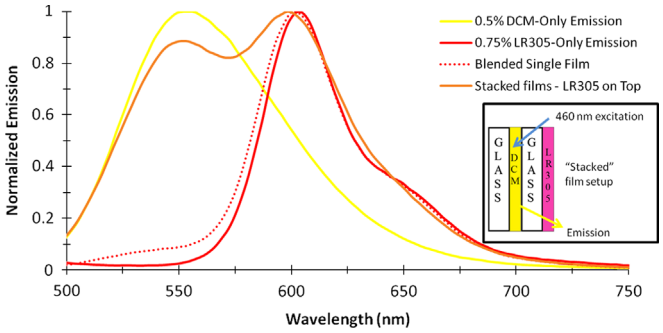

Fig. 4. Comparison of the emission spectra of stacked and blended LR305/DCM 0.75%/0.5% PMMA films when excited with 460 nm light. The "blended single film" is a single layer containing both 0.75% LR305:PMMA and 0.5% DCM:PMMA. "Stacked" films (illustrated above) comprise single-dye films (0.75% LR305:PMMA on top, 0.5% DCM:PMMA on the bottom) physically stacked on top of one another, with the LR305 "acceptor" film closer to the detection and excitation source. As such, any DCM emission would necessarily pass through the full LR305 optical density. Despite this, the stacked films show strong DCM fluorescence while the blend shows almost none.

The data shown in Fig. 4 are taken from films of like composition: approximately 5 μm thick "doctor-bladed" films on silicate glass, with PMMA as the host polymer as described. The single dye DCM and LR305 films have dye:polymer ratios of 0.5% and 0.75% by weight, respectively. The blended dye film has the same amount of each dye as in the single films, that is 0.5% DCM:PMMA and 0.75% LR305:PMMA by weight, for a total dye concentration of 1.25% dye:polymer. Stacked film emission data were taken by placing the two single dye films on top of one another, with the LR305 film above the DCM. The film emission spectra were taken with 460 nm excitation. As such, any DCM emission would necessarily pass through the LR305 film's entire optical density before being detected. The LR305 film was measured to be approximately 5 μm in thickness with a Dektak surface profiler, with a peak decadic absorbance of 0.166. In Ref. [21], LR305 was found to have a Naperian (natural logarithm) peak absorbance coefficient of 0.101 $ppm^{-1}\,cm^{-1}$ (where a "part per million" was defined as 10^{-4}% by weight in the host), which converts to approximately 0.0439 decadic absorbance units per percent by weight per micron thickness, agreeing with our 5 μm thickness measurement.

Although a small portion of the DCM emission is absorbed passing though the LR305 film, the stacked film emission stands in stark contrast to that of the blend. In both the stacked and blended films, the additive absorbance spectra are seen, as expected from the Beer–Lambert law. Likewise, the emission spectrum of the stacked films under 460 nm excitation closely matches their independent superposition; however the blend shows almost entirely acceptor emission. It should also be noted that DCM emission in the blend will, on average, pass through half the optical density of the LR305 film, assuming a uniform distribution of dopants, further highlighting a nonradiative donor quenching mechanism in the blend.

There are several mechanisms by which energy transfer may occur between fluorescent dye molecules. Radiative energy transfer, or emission of a photon by a donor chromophore and its subsequent reabsorption by the acceptor, can occur over macroscopic distances. Large spectral overlap between the absorption spectrum of LR305 and DCM's emission suggests that radiative energy transfer will occur to some extent if the dyes are placed in close proximity; however, when the relative intensities of the DCM and LR305 fluorescence peaks are compared between the blended dye film and the stacked films, the radiative processes are shown not to be the dominant energy transfer mechanism. Two well known mechanisms responsible for nonradiative energy transfer in fluorescent molecules in a rigid polymer matrix or viscous solvent (where collisional energy transfer can be neglected) are Dexter Excitation Transfer [27] and Förster Resonance Energy Transfer. Both operate in distinct distance regimes. Dexter Excitation Transfer (also referred to as exciton diffusion) stems from a physical overlap of donor and acceptor electron wavefunctions and operates over distances less than 20 Å. Considerations of Dexter Excitation Transfer (DET) are outside the scope of the samples studied in this work, as FRET is based on near-field fluorescence dipole interactions, and for samples with appreciable spectral overlap and random orientations (in other words, a suitably large average acceptor cross section), FRET is expected to work on distance scales generally up to an order of magnitude greater. As such, DET is not expected to be the dominant mechanism in the concentration regimes surrounding the Förster critical distance, a useful figure of merit in Förster theory generally denoted as R_0, or the distance at which the rate of energy transfer from the donor to the acceptor fluorophore is equal to the rate at which the donor will decay from its excited state in the absence of the acceptor. This can also be described as the donor–acceptor pair distance at which energy transfer is 50% efficient, and is given as described by

$$R_0^6 = \frac{9000\ln(10)\kappa^2\phi_d}{128\pi^5 N n^4}\int_0^\infty F_d(\lambda)\varepsilon_a(\lambda)\lambda^4\ d\lambda \qquad (1)$$

where ϕ_d is the normalized donor fluorescence per unit wavelength, $\varepsilon_a(\lambda)$ is the molar extinction coefficient of the acceptor between λ and $\lambda+d\lambda$, n is the refractive index of the host medium, and N is Avogadro's number. κ^2 is the dipole orientation factor, here taken to be 0.476, which has been shown to be the value of the orientation factor for randomly distributed donor and acceptor molecules in a rigid polymer matrix [28]. This well known Förster "spectroscopic ruler" [29] relation can be explained by both classical [30] and quantum mechanical [31] treatment of dipole interactions, as noted in Ref. [32]. Taking a donor quantum yield of 76% for DCM (ϕ_d), and using an overlap integral numerically determined to be $6.15\times10^{-14}\,\mathrm{cm^3\,M^{-1}}$ from the data used to generate Fig. 2, we obtain a critical FRET distance of 39.8 Å between DCM and LR305 in PMMA. In the case of the 0.75%/0.5% LR305/DCM blend, a convenient way to see the benefit afforded by the LR305 emission intensity is by observing the fluorescence intensity of LR305's emission peak (604 nm) as the excitation wavelength is varied. Without the DCM present, the LR305 peak emission intensity scales with the LR305's absorption spectrum as a function of excitation wavelength. Below 540 nm, the benefit from the added absorption of DCM is clearly seen (Fig. 5). Because the optical densities of the films are too low for large reabsorption of DCM emission by the LR305 (as seen experimentally in Fig. 4 and calculable from the low optical density of the films), we surmise that the enhanced emission is thus due to FRET and that the blue response of low optical density LR305 is efficiently enhanced without the additional escape cone and quantum yield losses of added emission and reabsorbtion events.

Total dye:polymer concentration was varied at two fixed LR305:DCM ratios: 1:2 LR305:DCM and 3:2 LR305:DCM (by weight). Fluorescence intensities of the blends are compared against the films containing only the donor at several representative concentrations (Figs. 6 and 7). By comparing the ratio of the donor fluorescence intensity in the presence of the acceptor to its intensity in the acceptor's absence, it is possible to estimate the transfer efficiency from Förster's relations:

$$E = 1 - \frac{F_{DA}}{F_D} \tag{2}$$

Using the critical distance, R_0, calculated from spectroscopic data and Eq. (1), we can then estimate the donor–acceptor separation according to Ref. [16]:

$$E = \frac{R_0^6}{R_0^6 + r^6} \tag{3}$$

This dependence has also been experimentally confirmed [29, 33]. Förster's theory predicts an r^{-6} dependence on transfer efficiency; using this relation to plot pair distance as a function of concentration, we recover the $-1/3$ power relationship between molecular spacing and concentration expected from dimensional analysis at both tested donor:acceptor ratios (Fig. 8). Unless the concentration of the donor is high enough for homotransfer to nonradiatively transport an exciton through a donor network to an acceptor site, donor quenching should be determined by the prevalence of acceptors. In both tested concentration ratios, the critical distance is calculated to fall in the regime of 0.2% acceptor dye (LR305) by weight, which for the LR305 dye is approximately 2×10^{-3} molal in PMMA, in agreement with the expected 10^{-3} M regime discussed in [14]; PMMA has a density on the order of 1 g per cubic centimeter.

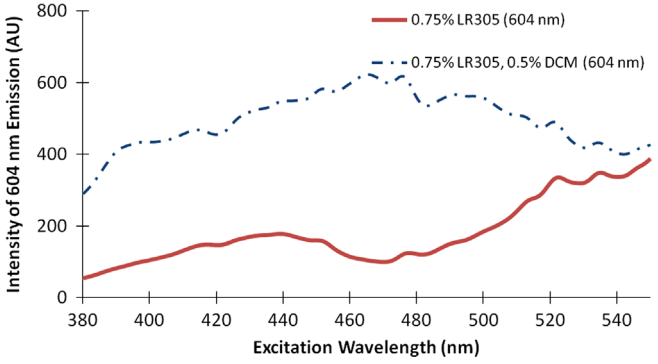

Fig. 5. Plot of the 604 nm emission intensity as excitation wavelength is swept across the absorption range of LR305 and DCM. The blended film shows enhanced LR305 emission response in the range of DCM's absorption. Intensities given in relative but arbitrary units.

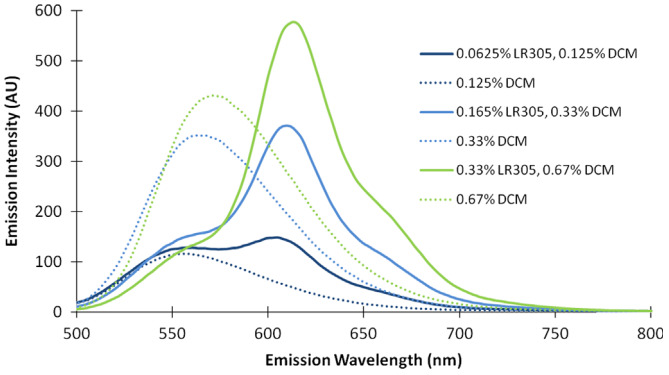

Fig. 6. Sample non-normalized emission profiles of 1:2 weight ratio LR305/DCM films under 460 nm excitation. DCM emission is quenched as concentration rises. Intensities given in relative but arbitrary units.

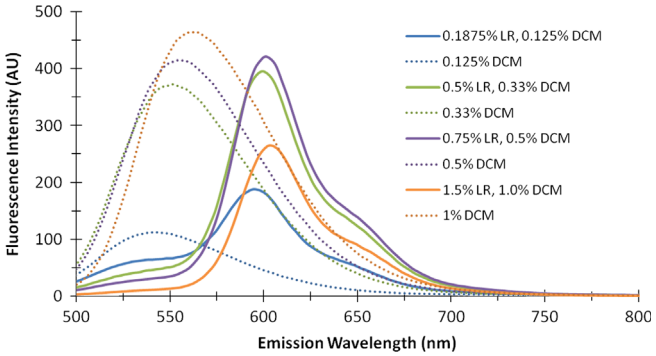

Fig. 7. Sample non-normalized emission profiles of 3:2 weight ratio LR305/DCM films under 460 nm excitation. The same effect is again seen.

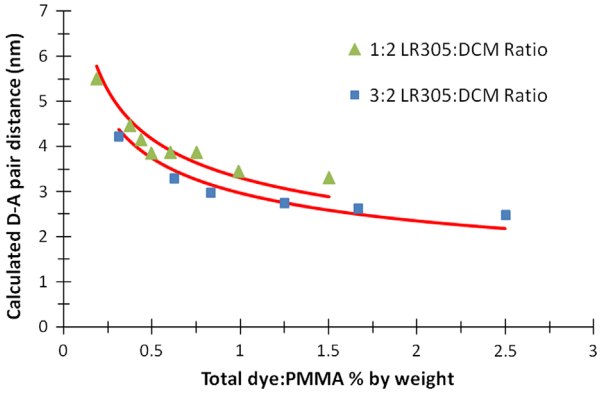

Fig. 8. Recovery of approximate $\{\text{concentration}\}^{-1/3}$ intermolecular distance from least squares fit of leading coefficient to calculated D–A pair distances. The fitted curves are least squares power law fits with the exponent fixed at $-1/3$ such that the leading coefficient of the form $\text{separation}=\{\text{concentration}\}^{-1/3}$ is fit to the data.

4. Benefit to luminescent solar concentrators

Even assuming unity quantum yield, no emission reabsorption, and no scattering from the host material, LSCs are fundamentally limited by the fraction of the solar spectrum that they absorb (Q_a from Ref. [3]). One of the desirable characteristics of Lumogen Red 305 is that its absorption spectrum extends into the blue, with a "secondary" absorption peak around 440 nm. This, coupled with its high quantum yield, good stability and commercial availability are what make it attractive as an LSC material. At sufficient optical by large densities, LR305 is capable of absorbing 25% or more of the air mass 1.5 power spectrum, with $>95\%$ absorption across the visible range below 600 nm.

With only Lumogen Red 305, however, achieving high absorption in the blue comes at the cost of greatly increased self-absorption. For example, 90% absorption at the 440 nm peak also means $\sim$75% absorption at 604 nm – the peak of the molecular emission spectrum. Extrapolating the measured absorbance spectrum of LR305 to 575 nm (peak) optical densities of between 0.5 and 4 decadic absorbance units and converting to transmission, the effect on self-absorption is immediately notable when compared to LR305's molecular emission spectrum (Fig. 9). As the transmission spectrum of LR305 approaches zero across its absorption range, progressively less of the air mass 1.5 power spectrum is absorbed for a fixed percentage optical density increase. For example, a sample with an absorbance peak of 0.1 will absorb $\sim$2.9% of AM1.5 power. Doubling the optical density for a peak absorbance of 0.2 captures 5.5–90% increase, but doubling optical densities from 2 to 4 absorbance units provides a much more modest 20% gain. The trend may be useful to visualize: Fig. 10 plots the percent of AM1.5 power absorbed versus peak optical density for an LR305 PMMA film, using the air mass 1.5 reference solar spectral irradiance published by the National Renewable Energy Laboratory. The gains come mostly from increased absorption in the blue, but at the expense of simultaneously raising the film's self-absorption, which continues to grow with optical density as the absorption spectrum saturates in the blue and progressively less solar power is absorbed for a given increase of optical density. With the addition of DCM, high blue absorption and enhanced LR305 emission from such excitation – can be achieved without altering the film's transmission appreciably at 604 nm,and making films at concentrations where FRET has been shown to be dominant eliminates the additional reabsorption and reemission losses associated with radiative dye transfer and self-absorption of the shorter wavelength dye. As a consequence of FRET, one is able to fully saturate the short wavelength dye's absorption without altering that of the emissive dye. In the context of two example films, 0.75% LR305 and 0.5%

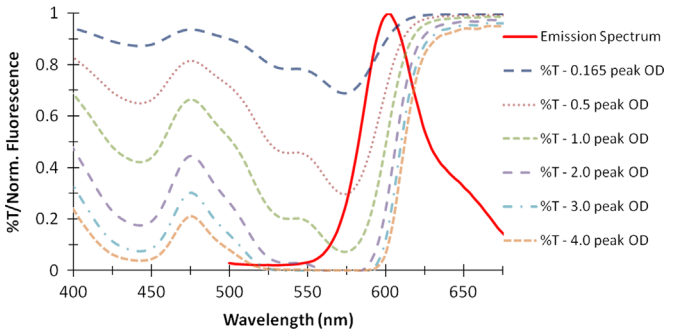

Fig. 9. Increases in the 575 nm (peak) optical density of L305 provides progressively less benefit to AM1.5 absorption, at the expense of greatly increased self-absorption of emitted light. Transmission at given peak optical density is plotted against LR305's own emission to highlight the increase in self-absorption in high optical density LR305 films.

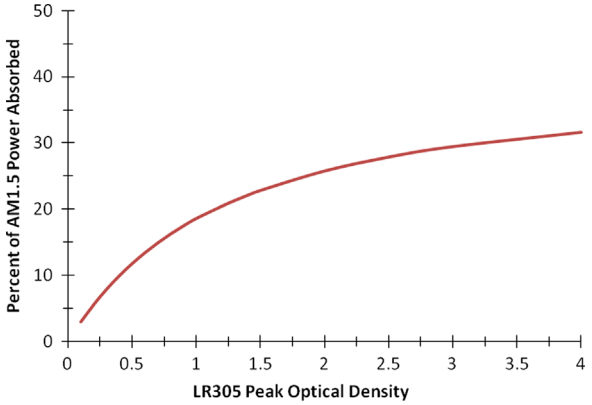

Fig. 10. Percentage of AM1.5 intensity spectrum absorbed by an LR305 film as a function of its peak optical density. Higher optical density films continue to increase self-absorption with progressively less solar photon flux absorption.

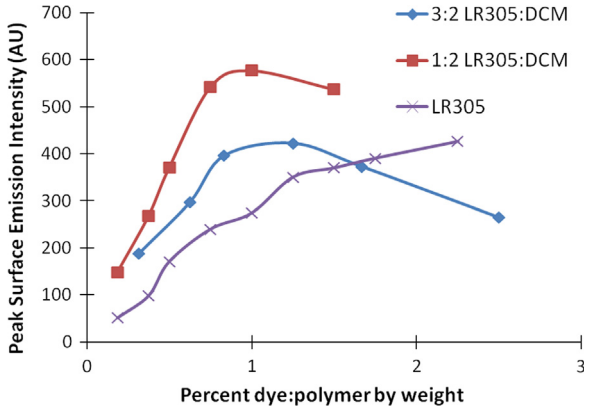

Fig. 11. Comparison of the peak fluorescence intensity of DCM blended and LR305 only films in different ratios as the concentration is varied. Lower acceptor:donor ratios allow for less self-absorption of emitted light, reducing the inner filter effect and facilitating brighter surface fluorescence.

DCM dye:PMMA ratio by weight, each absorbs 4.9% and 5.8% of AM1.5 power, respectively, with the blended film absorbing 11.15% of the power of the AM1.5 spectrum. Absorbing the same power from LR305 alone would require tripling its optical density, an effect which will carry forward to the portion of its absorbance overlapping the emission and drastically increase its self-absorption.

A simple way to see an effect of this is by examining the self-absorption or inner filter effect [34, 35]]35] as the concentration of the film is increased at the two tested LR305:DCM ratios and compared against pure LR305. At very low optical densities, fluorescence intensity can be expected to be proportional to absorbance. However, above optical densities of about 0.1 at the excitation and/or emission wavelengths, fluorescence intensity begins to deviate – see, for example Fig. 3 in Ref. [35] or [16]. Fig. 11 shows the peak fluorescence intensities observed with identically prepared films when excited at 460 nm. The blend with the larger amount of DCM shows a higher fluorescence peak intensity since the emissive side of the inner filter effect is lower for a given 460 nm optical density. Likewise, this peak is achieved at a lower concentration of both total dye and LR305 – resulting in lower self-absorption. While these ratios have not been optimized against a particular LSC panel geometry and total AM1.5 absorption, it illustrates the advantage that FRET may provide LSC films in considering future work.

Another advantage owing to efficient transfer between multiple dyes in the LSC film is color tunability. Perceived color of the film is determined solely by the transmitted light, and fluorescence is shown to have very little impact on measured transmission. Comparing transmission spectra of a 0.16 peak absorbance LR305 film from the thin film measurement system with that taken in a dual-monochrometer absorbance spectrometer, we see that there is little perceivable difference in the measured transmission of the film (Fig. 12). While the former setup uses a simulated D65 light source with appropriate background subtraction and should collect transmission and fluorescence of the film, the latter will minimize detected fluorescence as transmission at any given wavelength is measured under a narrow bandwith excitation rather than a D65 spectrum. If film fluorescence were to have a measurable impact, we would expect to see the fluorescence of the Lumogen dye above the transmission baseline in the thin film system measurement between 600 and 650 nm; any gain is not discernible from the noise floor of the measurement. The acceptance cone of the optical fiber used in the thin film measurement system may reduce the measured impact of fluorescence on transmission; while an area surface element of the film will fluoresce into its escape cone, the acceptance cone of the optical fiber is likely smaller [21]. However, a real observer at a distance from the LSC material would also observe limited fluorescence angles from a fixed area element of the film.

Thus we can reasonably argue that while fluorescence cannot generally be neglected in determining color [36, Section 3.7], in the case of planar LSC films we can consider only absorption, and film color tunability is calculable from the additive absorbance of multiple dyes. The addition of DCM shifts the pink–red range of LR305 films towards orange; however using as few as three appropriately absorbing dyes, a large portion of the visible spectrum may be covered. Film color can be predicted according to a subtractive scheme such as the CMY color model. Fig. 13 shows various color possibilities achievable, in a CIE1931 chromaticity diagram with data taken from the thin film measurement system. The figure includes data from the single LR305 dyes, the blended LR305 and DCM dye films, LR305 with a red absorber (LD700 Perchlorate, excition chemical co.), and LR305 with a dielectric bragg reflector placed in front of the film at various angles to simulate different absorbance spectra. Efficient FRET becomes increasingly important as more dyes are used in order to minimize waveguide efficiency losses (losses from reduced Q_c, as described in Ref. [3]).

5. Conclusion

This research was oriented towards the goal of increasing single-layer LSC efficiency. We have established the concentration regime in a PMMA matrix where FRET becomes the dominant transfer mechanism between two luminescent dyes. We have provided an illustration of how this might be exploited to increase AM1.5 power absorption of a given film without altering self-absorption. Investigation of the minimum concentrations necessary for FRET will aid future LSC design, and allow for tunable absorption spectra while minimizing the detriment to waveguide efficiency from self-absorption. Moreover, the potential applications for efficient light downconversion mechanisms within a waveguide extend beyond the scope of our stated goals.

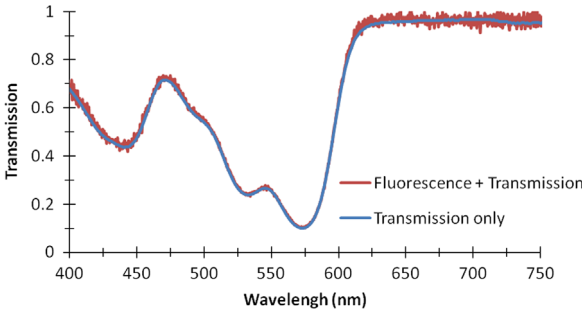

Fig. 12. Comparison of transmitted light both with (thin film measurement system) and without (dual-monochrometer UV–vis spectrometer) fluorescence intensity included.

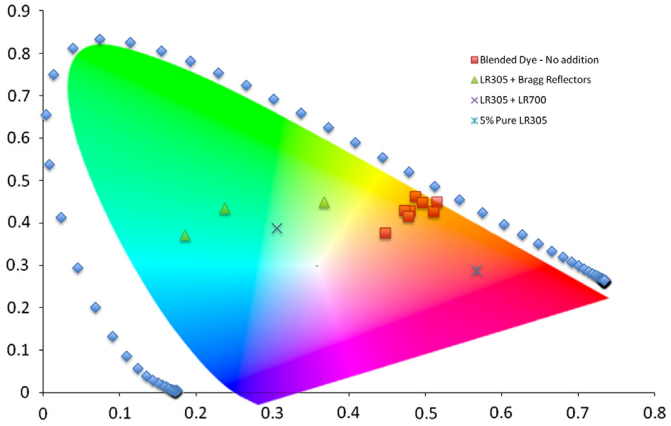

Fig. 13. Various color possibilities are plotted on a CIE 1931 *Xy* chromaticity diagram. CIE 1931 *Xy* chromaticity may be derived from CIE *XYZ* colorspace values from a suitable transformation. (For interpretation of the references to color in this figure legend, the reader is referred to the web version of this article.)

References

[1] G. Keil, Journal of Applied Physics 40 (9) (1969) 3544.
[2] G. Seybold, G. Wagenblast, Dyes and Pigments 11 (4) (1989) 303.
[3] W.H. Weber, J. Lambe, Applied Optics 15 (10) (1976) 2299.
[4] A.M. Hermann, Solar Energy 29 (4) (1982) 323.
[5] M.G. Debije, P. Verbunt, Advanced Energy Materials 2 (1) (2012) 12.
[6] J.S. Batchelder, A.H. Zewail, T. Cole, Applied Optics 18 (18) (1979) p3090.
[7] D. Avnir, D. Levy, R. Reisfeld, Journal of Physics and Chemistry 88 (1984) 5956.
[8] V. Sholin, J.D. Olson, S.A. Carter, Journal of Applied Physics 101 (2007) 123114.
[9] M.G. Hyldahl, S.T. Bailey, B.P. Wittmershaus, Solar Energy 83 (4) (2009) 566.
[10] M.J. Currie, J.K. Mapel, T.D. Heidel, S. Goffri, M.A. Baldo, Science 321 (5886) (2008) 226.
[11] C. Mulder, P. Reusswig, A. Velázquez, H. Kim, C. Rotschild, M. Baldo, Optics Express 18 (2010) A79.
[12] C. Mulder, P. Reusswig, A. Velázquez, H. Kim, C. Rotschild, M. Baldo, Optics Express 18 (2010) A91.
[13] S. Woei Leow, C. Corrado, M. Osborn, M. Isaacson, G. Alers, S.A. Carter, Journal of Applied Physics 113 (21) (2013).
[14] B.A Swartz, T. Cole, A.H. Zewail, Optics Letters 1 (2) (1977) 73.
[15] S.T. Bailey, G.E Lokey, M.S. Hanes, J. Shearer, J.B. McLafferty, G.T. Beaumont, T.T. Baseler, J.M Layhue, D.R. Broussard, Y. Zhang, B.P. Wittmershaus, Solar Energy Materials 91 (2007) 67.
[16] J.R. Lakowicz, Principles of Fluorescence Spectroscopy, third ed., Springer Science and Business Media, New York, 2006.
[17] A. Yekta, J. Duhamel, M.A. Winnik, Chemical Physics Letters 235 (1995) 119.
[18] O.J. Rolinski, D. Birch, Journal of Chemical Physics 112 (20) (2000) 8923.
[19] J.S. Batchelder, A.H. Zewail, T. Cole, Applied Optics 20 (21) (1981) 3733.
[20] J. Sansregret, J.M. Drake, W.R.L. Thomas, M.L. Lesiecki, Applied Optics 22 (4) (1983) 573.
[21] L.R. Wilson, B.C. Rowan, N. Robertson, O. Moudam, A.C. Jones, B.S. Richards, Applied Optics 49 (9) (2010) 1651.
[22] Solar Photovoltaics: Status, Costs, and Trends. EPRI, Palo Alto, CA, 2009, 1015804.
[23] C. Corrado, S.W. Leow, M. Osborn, E. Chan, B. Balaban, S.A. Carter, Solar Energy Materials and Solar Cells 111 (2013) 74.
[24] J.M. Drake, M.L. Lesiecki, D.M. Camaioni, Chemical Physics Letters 113 (6) (1985) 530.
[25] S.L. Bondarev, V.N. Knyukshto, V.I. Stepuro, A.P. Stupak, A.A. Turban, Journal of Applied Spectroscopy 71 (2) (2004) 194.
[26] L.R. Wilson, B.S. Richards, Applied Optics 48 (2) (2009) 212–220.
[27] D.L. Dexter, Journal of Chemical Physics 21 (5) (1953) 836.

[28] I.Z. Steinberg, Annual Review of Biochemistry 40 (1971) 83.
[29] L. Stryer, R.P. Haughland, Proceedings of the National Academy of Sciences of the United States of America 58 (1967) 719.
[30] T. Förster, Fluoreszenz OrganischerVerbindungen, Vandenhoeck and Ruprecht, Göttingen, 1951.
[31] T. Förster, Annalen der Physik 437 (1948) 55.
[32] D. Valeur, M. Berberan-Santos, Molecular Fluorescence: Principles and Applications, second edition., Wiley-VCH Verlag GmbH and Co. KGaA, Weinheim, 2012.
[33] G. Gabor, Biopolymers 6 (1968) 809.
[34] C.A. Parker, W.T. Rees, Analyst 87 (1031) (1962) 83.
[35] M. Kubista, R. Sjöback, S. Eriksson, B. Albinsson, Analyst 119 (1994) 417.
[36] Gaurav Sharma, Raja Bala, Digital Color Imaging Handbook, CRC Press, Boca Raton, 2002.